Influence of Hydrogen and Test Frequency on Fatigue Crack Path

Yukitaka Murakami[1] and Saburo Matsuoka[1]

[1] Kyushu University and The Research Center for Hydrogen Industrial Use and Storage (HYDROGENIUS), AIST, 744 Moto-Oka, Nishi-ku, Fukuoka, 819-0395 JAPAN
ymura@mech.kyushu-u.ac.jp

ABSTRACT. *The present paper overviews the recent progress on HE obtained at HYDROGENIUS. The influence of hydrogen and strong test frequency on fatigue crack path is discussed with a particular attention. The mechanism of change in fatigue crack path depending on test frequency is explained by the coupled effect of hydrogen induced localized plasticity at crack tip and test frequency.*

The test frequency of the fatigue test was switched from f = 2 Hz to f = 0.02 Hz and the crack growth behaviour was observed by the replica method. These two step fatigue tests were repeated and the variation of the crack growth behaviour by switching the test pattern from f = 2 Hz to f = 0.02 Hz was investigated.

Particularly important phenomena are the localization of fatigue slip bands and also strong frequency effects on fatigue crack growth rates. For example, with a decrease in frequency of fatigue loading down to the level of 0.02 Hz, the fatigue crack growth rate of a Cr-Mo steel was accelerated by 10 - 30 times. The same phenomenon also occurred even in austenitic stainless steels at the frequency of the level of 0.001 Hz. Striation morphology was also influenced by hydrogen.

The crack path of the hydrogen-uncharged specimen was monotonic and showed no particular variation even after switching the test frequency from f = 2 Hz to 0.02 Hz and also 0.02 Hz to 2 Hz. The monotonic moderate curving of the crack path was caused by the growth of plastic zone size due to increase in the crack length, i.e. the stress intensity factor range. Namely, the plane stress condition is gradually satisfied and the crack extension by shear mode ahead of crack tip becomes dominant near specimen surface. On the other hand, the crack of hydrogen-charged specimen grew in the inclined direction under f = 2 Hz, though the crack grew straight under f = 0.02 Hz.

INTRODUCTION

In order to enable the “hydrogen society (or hydrogen economy)” in the near future, a number of pressing technical problems must be solved. One important task for mechanical engineers and material scientists is the development of materials and systems which are capable of withstanding the effects of cyclic loading in hydrogen environments. In the past much research has been concentrated on the phenomenon

known as hydrogen embrittlement [1-3]. Hydrogen effects on slip localization [2-4], softening and hardening [4-12], hydrogen-dislocation interactions [12-14] and creep [15] have been also reported. However, most research on HE over the past 40 years has paid insufficient attention to two points that are crucially important in the elucidation of the true mechanism. One is that, in most studies, the hydrogen content of specimens was not directly measured. Second, detailed studies that have quantified the influence of hydrogen on fatigue crack growth behaviour, based on microscopic observations are very rare; most studies have only examined the influence of hydrogen on tensile properties[16-33]. In order to produce components which must perform satisfactorily in service for up to 15 years, there is an urgent need for basic, reliable data on the fatigue behaviour of candidate materials in hydrogen environments.

Two typical fuel cell (FC) systems are the stationary FC system and the automotive FC (Fuel Cell Vehicle, FCV) system. In the FCV system, many components such as the liner of high pressure hydrogen storage tank, valves, pressure sensors, hydrogen accumulators, pipes, etc, are exposed to high pressure hydrogen environment for a long period up to 15 years. Sufficient data have not been obtained on the content of hydrogen which diffuses into metals during a long period of exposure to hydrogen. “How much hydrogen is contained in components in the fuel cell related system?” is a very important question. But this question is difficult to answer.

MATERIALS AND EXPERIMENTAL METHODS

Materials and specimens

The material used in this study is a Cr-Mo steel JIS SCM435. Table 1 shows the chemical compositions and the Vickers hardnesses (Load: 9.8 N) of these materials. Hydrogen contents were measured by the thermal desorption spectrometry (TDS) using a quadruple mass spectrometer. The measurement accuracy of the TDS is 0.01 wppm. Figures 1(a) and (b) show the fatigue specimen dimensions and the dimensions of the small hole which was introduced into the specimen surface. After polishing with #2000 emery paper, the specimen surface was finished by buffing using colloidal SiO2 (0.04 mm) solution. A small artificial hole, 100 μm diameter and 100 μm deep, was drilled into the specimen surface as a fatigue crack growth starter. In the hydrogen-charged specimens, the specimen surface was buffed after hydrogen charging, and the hole was then introduced immediately.

Table 1 Chemical composition (w%, *wppm) and Vickers hardness *HV*

	C	Si	Mn	P	S	Ni	Cr	Mo	Cu	*HV*
SCM435	0.37	0.18	0.78	0.025	0.015	0.09	1.05	0.15	0.1	330

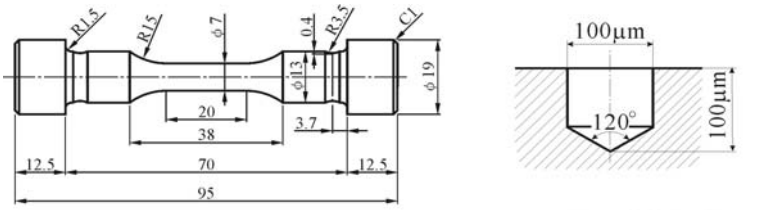

(a) Tension-compression specimen (b) Small artificial hole

Figure 1. Dimensions of the fatigue test specimen and drilled hole

Method of hydrogen charging

Hydrogen was charged into the specimens of SCM435 by soaking them in a 20% ammonium thiocyanate solution (NH4 SCN).

Method of fatigue testing

Fatigue tests of the hydrogen-charged and uncharged specimens were carried out at room temperature in laboratory air. The fatigue tests for SCM435 were conducted at a stress ratio $R = -1$ and at a testing frequency between 0.02 Hz and 20 Hz.

Following the fatigue tests, in order to measure the hydrogen content remaining in specimens, 0.8 mm thick disks were immediately cut from each specimen, under water-cooling. Then, hydrogen contents of disks were measured by TDS. Measurements were carried out up to 800 °C at a heating rate of 0.5 °C/s.

RESULTS AND DISCUSSION

The basic mechanism of void growth in tensile test

The hydrogen-charged specimens show a peculiar void growth inside the specimen in tensile test. Figure 2 shows an interesting difference of void growth behaviour between the uncharged specimen (Fig. 2(a)) and the hydrogen-charged specimen (Fig. 2(b)). The basic mechanism of the void growth lateral to tensile axis in the hydrogen-charged specimen (Fig. 2(b) and (c)) can be considered consistent with that of fatigue crack growth(Fig. 9).

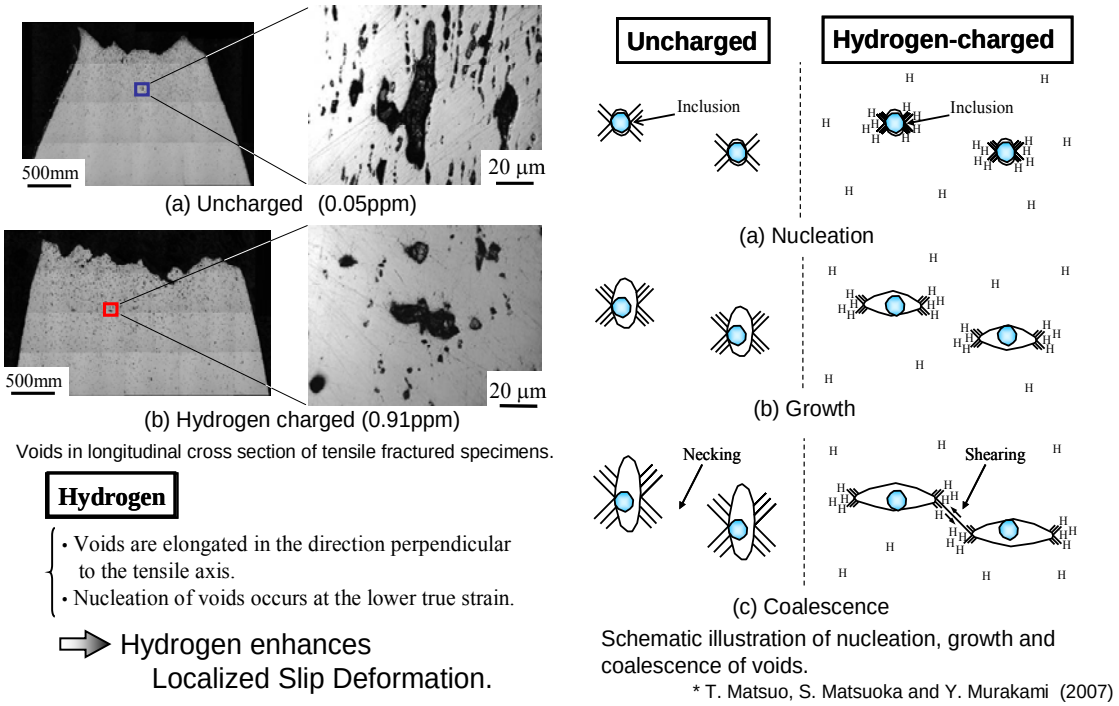

Figure 2. Development of voids in tensile test of the hydrogen charged specimen of a pipe line steel, JIS-SGP (0.078% carbon steel)[34]

Effect of Hydrogen on Fatigue Behaviour of Cr-Mo steel SCM435

Cr-Mo steel: JIS SCM435 is a candidate material for the hydrogen storage cylinder of hydrogen station equipped with 35MPa hydrogen supply to FCV. The effect of hydrogen on fatigue crack behaviour of SCM435 was investigated in details by H. Tanaka et al [35]. In this paper, a part of their work will be introduced.

Figure 3 shows the relationship between crack length a and number of cycle N under the tension- compression stress amplitude σ_a = 600 MPa. The fatigue crack growth rate da/dN of the hydrogen charged specimens is much higher than the uncharged specimens. Another important point is that da/dN increases with decreasing test frequency. It is presumed that there is sufficient time for hydrogen to diffuse and concentrate at crack tip under low test frequency.

Figure 4 shows the relationship between da/dN and stress intensity factor range ΔK. Figure 5 shows the relationship between the acceleration of crack growth rate defined by the ratio of da/dN with hydrogen to da/dN in air and the test frequency f. The most important result in Figure 5 is that da/dN at ΔK < 17MPa $\sqrt{}$m (da/dN = 1.0×10^{-8}m/cycle -1.0×10^{-7}m/cycle) and f < 2Hz for the hydrogen charged specimens are merged into one line regardless of the value of f and the crack growth rates under these conditions are 30 times higher than those for uncharged specimens.

This frequency tendency can also be confirmed by Fig. 5. This tendency can be explained as follows. At very low crack growth rate da/dN <1.0×10^{-7}m/cycle, hydrogen

has sufficient time to diffuse into the crack tip process zone, because the location of crack tip does not move so much distance toward the direction of crack extension and the crack tip stays inside the process zone until hydrogen concentrates. On the other hand, for da/dN $>1.0\times10^{-7}$m/cycle, it is presumed that crack passes the process zone at crack tip before hydrogen concentrates and the rate of acceleration of da/dN varies depending on test frequency. However, regardless of the values of frequency, da/dN of hydrogen charged specimens gradually merges to the line of da/dN of uncharged specimens at higher value of da/dN, because crack grows much faster than hydrogen diffusion to crack tip. Thus, the crack growth rate and hydrogen effect are mutually coupled.

The dotted line of Fig. 4 shows approximately 30 times acceleration of fatigue crack growth rate in presence of hydrogen and can be considered to be the upper bound of hydrogen effect which should be used for the fatigue life prediction design of hydrogen storage cylinder.

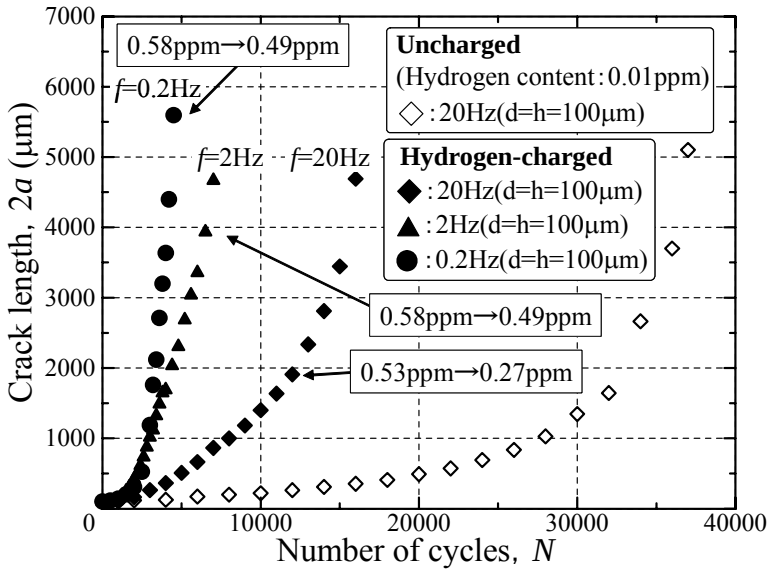

Figure 3. Relationship between crack length 2a and number of cycles N. σ_a = 600 MPa. Material: SCM435 (H. Tanaka, et al[40])

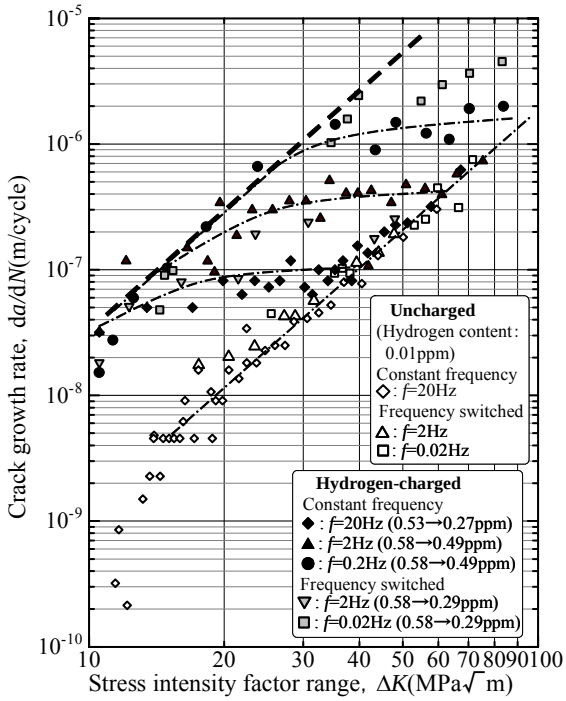

Figure 4. Relationship between da/dN and ΔK. Material: SCM435 (H.Tanaka, et al[40])

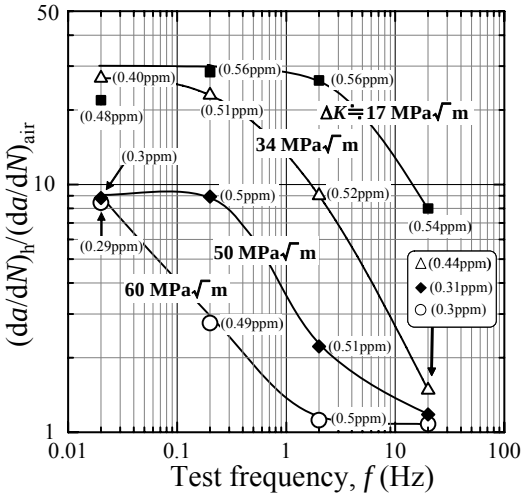

Figure 5. Relationship between acceleration of crack growth rate $(\mathrm{d}a/\mathrm{d}N)_h/(\mathrm{d}a/\mathrm{d}N)$ air and frequency f. Material: SCM435 (H. Tanaka, et al[40])

Figure 6 shows the crack shapes and slip bands morphologies. The crack of the hydrogen charged specimen looks thinner than the uncharged specimens. The crack paths of the hydrogen charged specimens tested under f = 0.2 and 2Hz are relatively more linear than those of the uncharged specimens and also that of the hydrogen

charged specimen tested under f = 20Hz. The crack tip of the uncharged specimen has many slip bands spreaded broad beside the crack line. On the other hand, the slip bands of the hydrogen charged specimens are localized only at very narrow area beside the crack line. Kanezaki, et al [36] reported the same slip localization at crack tip and linear crack path in the fatigue of hydrogen charged austenitic stainless steels.

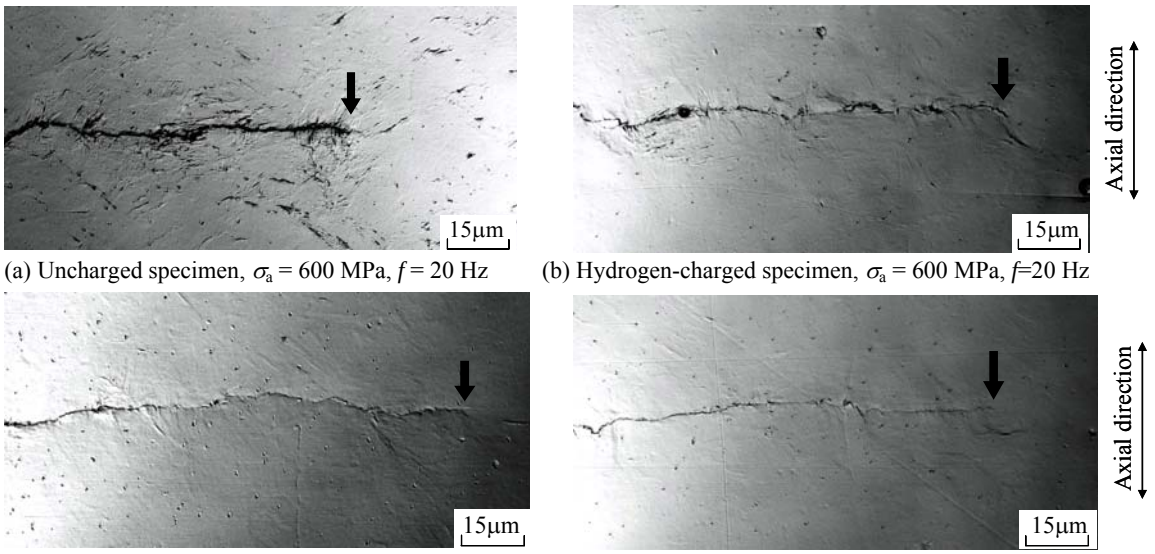

(a) Uncharged specimen, σ_a = 600 MPa, f = 20 Hz (b) Hydrogen-charged specimen, σ_a = 600 MPa, f=20 Hz

(c) Hydrogen- charged specimen, σ_a = 600 MPa, f = 2 Hz (d) Hydrogen-charged specimen, σ_a = 600 MPa, f = 0.2 Hz

Figure 6. Slip bands and fatigue cracks in uncharged and hydrogen-charged specimens at $\Delta K \fallingdotseq 20$ MPa$\sqrt{\text{m}}$. Material: SCM435 (H. Tanaka, et al [40])

In order to make clear the mechanism of slip bands localization and linear crack path more in details, the following fatigue tests were carried out.

1. First, the fatigue test was carried out at f = 2Hz and the crack growth behaviour was observed by the replica method.
2. Second, the test frequency of the fatigue test was switched to f = 0.02Hz and the crack growth behaviour was observed by the replica method.

These two step fatigue tests were repeated and the variation of the crack growth behaviour by switching the test pattern from 1 to 2 was observed. The results of these tests were very interesting as described in the following.

Figures 7(a) and (b) show the overall crack growth paths. The crack path of the uncharged specimens is monotonic and show no particular variation even after switching the test frequency from f = 2Hz to 0.02Hz and also from 0.02Hz to 2Hz. The monotonic moderate curving of the crack of Fig. 7(a) is caused by the growth of plastic zone size due to increase in a, i.e. ΔK. Namely, the plane stress condition is gradually satisfied and the crack extension by shear mode ahead of crack tip becomes dominant near specimen surface. Figure 8 explains this mechanism caused by subsurface plane strain condition and surface plane stress condition.

However, the crack of the hydrogen charged specimen for $\Delta K > 40\text{MPa}\sqrt{\text{m}}$, the influence of switching the test frequency appears very clearly in the variation of slip bands morphologies and crack path. The crack grows in the inclined direction under f = 2Hz, though the crack grows straight under f = 0.02Hz. Figure 7(c) is the magnification of the localization of slip bands in the region of f = 0.02Hz. As shown by the marks ■ and ▼ in Fig. 4, the da/dN under f = 0.02Hz in this region (■) is approximately 10 times faster than da/dN under f = 2.0Hz. The cause for the difference between the inclined crack growth for f = 2Hz and the linear crack growth for f = 0.02Hz can be interpreted as follows.

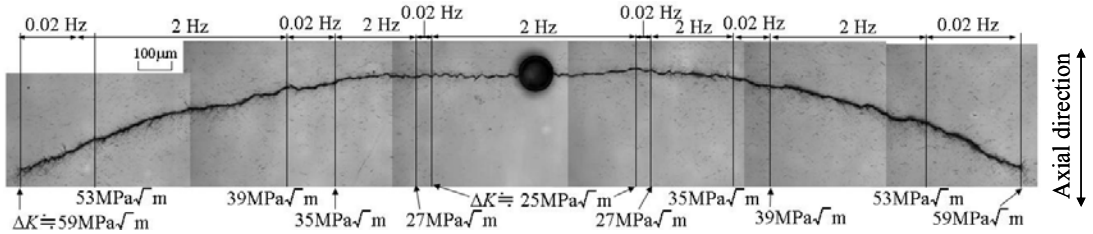

(a) Crack path in the uncharged specimen.

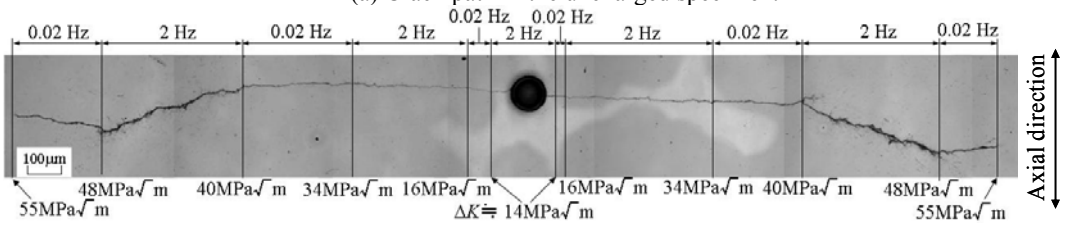

(b) Crack path in the hydrogen-charged specimen.

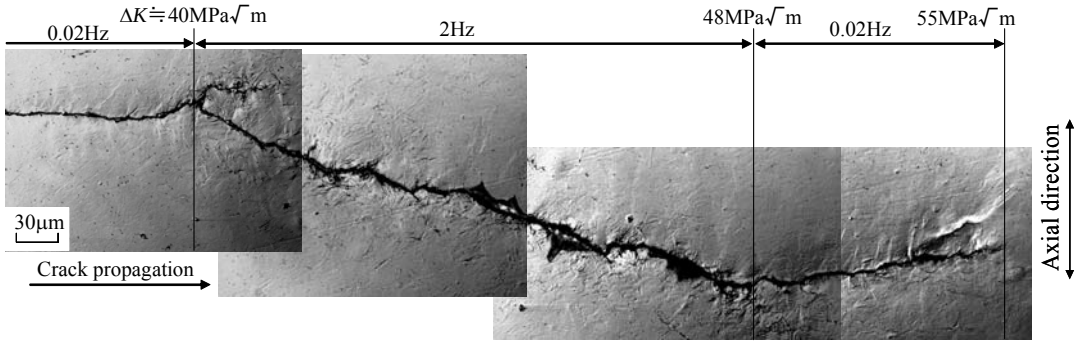

(c) Crack path and slip bands in the hydrogen-charged specimen

Figure 7. Fatigue crack path and slip bands for the test with two frequencies of 0.02 Hz and 2 Hz at σ_a = 600 MPa, Material: SCM435 (H, Tanaka, et al [40])

As explained with respect to Fig. 6, hydrogen influences the localization of slip band and decreases the plastic zone size at crack tip. As the test frequency f decreases, this hydrogen effect is enhanced, resulting the plane strain condition with smaller plastic zone size even at high ΔK.

Thus, the inclined crack growth behaviour under f = 2Hz in Fig. 7(b) and (c) is due to large plastic zone size with less hydrogen effect which is almost similar to the case of Fig. 7(a). It must be noted that these inclined cracks are made by shear mode fracture and are inclined to specimen surface (see the mechanism explained in Fig. 8).

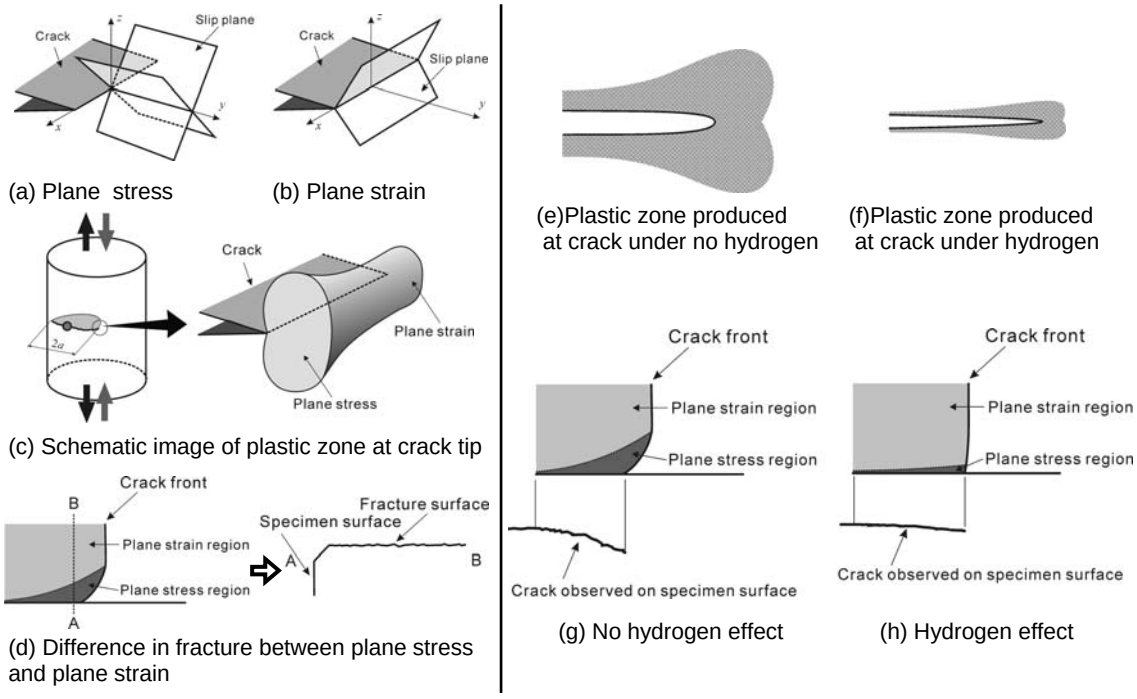

Figure 8. Hydrogen and frequency effects on plastic zone size

Hydrogen-induced striation formation mechanism

Based on the data for striation shape, which involves information on the crack growth mechanism, we will discuss the mechanisms of crack tip opening, crack growth, and decrease in H/s induced by hydrogen. We will also discuss the mechanisms related, not only to the mechanism of hydrogen embrittlement in fatigue, but also to the basic mechanism of hydrogen embrittlement in static fracture.

The distributions of maximum shear stress and of hydrostatic tensile stress, ahead of the crack tip, under plane strain can be easily calculated by the elastic solution of crack. In the case when there is no hydrogen, slip from the crack tip occurs in the 75.8° direction, where the shear stress has its maximum under plane strain. The slip in the 75.8° direction causes both crack tip blunting and crack growth at the initial stage of loading. Under a given load level crack tip blunting occurs as a crack grows and, finally, at the maximum load crack growth is saturated. This mechanism has been well known in previous studies on metal fatigue [37-40]. On the other hand, for the case when hydrogen is present, Sofronis et al. [41] showed, by numerical analysis of hydrogen diffusion near the crack tip, that hydrogen diffuses to, and concentrates at, the region

where the hydrostatic tensile stress has its maximum. Tabata, Birmbaum and et al. [18] suggested, through TEM observation of the interaction between dislocations and hydrogen, that yield stress decreases as a function of hydrogen pressure. Considering their experimental result, it is therefore presumed that yield stress decreases at a region where hydrogen concentrates. As a result, crack tip blunting and crack growth both occur during the whole load cycle. Namely, even if crack tip blunting occurs at a given load level that is below the maximum load, further slip takes place at the growing crack tip where hydrogen repeatedly concentrates. This further slip reduces crack tip blunting in the 75.8° direction; both crack tip blunting and crack growth occur in a coupled manner during the whole load cycle. As shown in Fig. 9, the fatigue crack growth mechanism of ductile materials is based on striations formed by slip at a crack tip. This differs from the static fracture mechanism of BCC metals. However, the diffusion and concentration behaviour of hydrogen near a crack tip, or near a notch root, is similar in both FCC and BCC metals. Furthermore, with decreasing fatigue test frequency, there is sufficient time for hydrogen to diffuse towards crack tips, and a large amount of hydrogen concentrates near crack tips. As a result, a crack continues to grow before the crack tip becomes fully blunt.

It is well known that there are three types of crack closure which control fatigue crack growth [43-45]. From the viewpoint of plasticity-induced crack closure [42], it follows from the above discussion that the amount of plastic deformation (plastic zone size) at the maximum load, *P*max, is smaller in the presence of hydrogen than in its absence. Figures 9(a) and (b) illustrate the effect of hydrogen on the crack closure mechanism during one load cycle. Figure 9(a-2) shows the crack opening behavior on the way to the maximum load in the absence of hydrogen. The crack tip opening displacement reaches its saturated value at a given load level and crack growth ceases. As shown in Fig. 9(b-2), however, hydrogen concentrates near the crack tip in the presence of hydrogen. Hydrogen concentration enhances further crack opening by slip, and crack growth continues. Since the corresponding plastic zone at the crack tip does not become large, the plastic zone wake which remains on the fracture surface is shallow. Figure 9(c) and (d) are schematic illustrations of plastic zone wakes with and without hydrogen. Ritchie et al. [46, 47] pointed out that the reason for the increase in crack growth rates of a Cr-Mo steel, in a hydrogen gas environment, is the increase in ΔK_{eff} due to the absence of oxide induced crack closure. However, as shown in Fig. 9, hydrogen influences all three types of crack closure mechanisms. In particular, the effect of hydrogen on plasticity-induced crack closure is crucially important for all three types of crack closure mechanism. This phenomenon results both in decrease in the height of striation and in decrease in the crack opening load (decrease in ΔK_{op} and increase in ΔK_{eff}).

As has been described in the previous paragraph, a crack grows continuously during loading, in the presence of hydrogen, even before the crack opening displacement reaches its maximum value. Consequently, the crack tip shape at the maximum load is sharper in the presence of hydrogen than in its absence. The effect of hydrogen on plastic deformation at a crack tip may be reduced during unloading. This is because the stress field at the crack tip becomes compressive. Nevertheless, it is presumed that the

vertical distance between the peak and the valley of a striation becomes small. This is because the crack opening displacement at the maximum load is small in the presence of hydrogen, even though the amount of reverse slip is the same as that in air. This is the possible mechanism for the small ratio of striation height, *H*, to spacing s, *H/s*, in the presence of hydrogen.

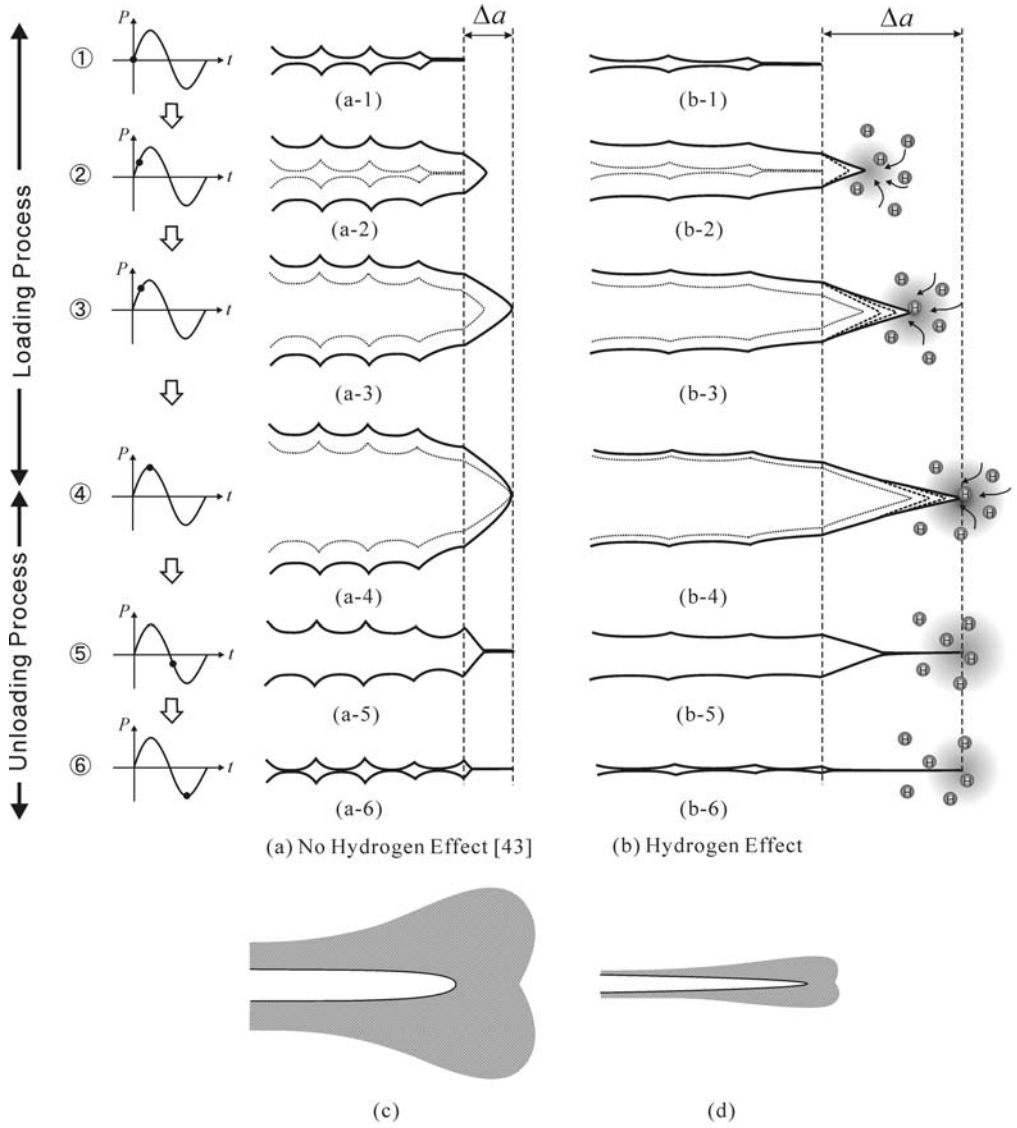

Figure 9. Crack tip opening and striation formation mechanism in fatigue: (a) no hydrogen effect, (b) hydrogen effect, (c) schematic image of thick plastic zone wake produced at a crack under no hydrogen, and (d) schematic image of shallow plastic zone wake produced at a crack under hydrogen effect[42].

CONCLUSIONS

The basic mechanism of hydrogen embrittlement in the fatigue of a Cr-Mo steel JIS SCM435, has been made clear on the basis of the effects of hydrogen and load frequency on fatigue crack growth rates. The conclusions can be summarized as follows.

(1) With decreasing load frequency, the fatigue crack growth rate for the hydrogen charged specimens increased significantly. However, there is the upper bound of the acceleration of da/dN and it is 30 times of da/dN for uncharged specimens.

(2) The two step fatigue tests for different load frequencies f = 2Hz and 0.02Hz made clear the mechanism of slip localization and linear crack path in the fatigue of hydrogen carged specimens. The fatigue crack path of uncharged specimens was monotonically inclined and curved regardless of load frequency due to the growth of plastic zone with increasing ΔK. However, the fatigue crack path of hydrogen charged specimens changed from a inclined and curved shape to a linear and straight crack by switching f from f = 2Hz to 0.02Hz. This is due to the slip localization and decrease in plastic zone size in presence of hydrogen.

ACKNOWLEDGEMENT

This research has been supported by the NEDO project "Fundamental Research Project on Advanced Hydrogen Science (2006-2012)".

REFERENCES

1. Farrell, K., Quarrell, A.G. (1964) *J. of the Iron and Steel Institute* 1002-1011.
2. Shih, D.S., Robertson, I.M., Birnbaum, H.K. (1988) *Acta Metall*. 36, 111-124.
3. Brass, A.M., Chene, J. (1998) *Material Sci. and Engng*. A242, 210-221.
4. Birnbaum, H.K., Sofronis, P. (1994) *Material Sci. and Engng.* A176, 191-202.
5. Heller, W.R. (1961) *Acta Metall.* 9, 600-613.
6. Matsui, H., Kimura, H. (1979) *Mater. Sci. Engng.* 40, 227-234.
7. Kimura, H., Matsui, H. (1979) *Scripta Metallurgica* 13, 221-223.
8. Hirth, J.P. (1980) *Metall. Trans.* A, 11A, 861-890.
9. Dufresne, J.F., Seeger, A., Groh, P., Moser, P. (1976) *Phys. Stat. Sol*. (a), 36, 579-589.
10. Senkov, O.N., Jonas, J.J. (1996) *Metall. Mater. Trans*. A, 27A, 1877-1887.
11. Au, J.J., Birnbaum, H.K. (1973) *Scripta Metallurgica* 7, 595-604.
12. Magnin, T., Bosch, C., Wolski, K., Delafosse, D. (2001) *Mater. Sci. Eng*. A314 7-11.
13. Clum, J.A. (1975) *Scripta Metallurgica* 9, 51-58.
14. Birnbaum, H.K., Robertson, I.M., Sofronis, P. (2000) In: *Multiscale Phenomena in Plasticity,* pp.367, Lepinoux, J. (Ed.), Kluwer Academic Publishers.

15. Mignot, F., Doquet, V., Sarrazin-Baudoux, C. (2004) *Mater. Sci. Eng*. A380, 308-319.
16. Troiano, A.R. (1960) *Trans. ASM* 52, 54-80.
17. Oriani, O.A., Josephic, P.H. (1974) *Acta Metall*. 22, 1065-1074.
18. Tabata, T., Birnbaum, H.K. (1983) *Scripta Metall.* 17, 947-950.
19. Robertson, I.M., Birnbaum, H.K. (1986) *Acta Metall.* 34, 353-366.
20. Vennett, R.M., Ansell, G.S. (1967) *Trans. ASM*. 60, 242-251.
21. Benson Jr, R.B., Dann, R.K., Roberts Jr, L.W. (1968) *Trans. Metall. Soc. AIME* 242, 2199-2205.
22. Lagneborg, R. (1969) *J. Iron and Steel Inst*. 207, 363-366.
23. Beachem, C.D. (1972) *Metall. Trans.* 3, 437-451.
24. Garber, R., Bernstein, I.M., Thompson, A.W. (1976) *Scripta Metall*. 10, 341-345.
25. Cialone, H., Asaro, R.J. (1979) *Metall. Trans.* 10A, 367-375.
26. Eliezer, D., Chakrapani, D.G., Altstetter, C.J., Pugh, E.N. (1979) *Metall. Trans.* 10A, 935-941.
27. Rosenthal, Y., M.-markowitch, M., Stern, A., Eliezer, D. (1981) *Scripta Metall*. 15, 861-866.
28. Singh, S., Altstetter, C. (1982) *Metall. Trans.* 13A, 1799-1808.
29. Stoltz, R.E., Moody, N.R., Perra, M.W. (1983) *Metall. Trans.*. 14A, 1528-1531.
30. Rozenak, P., Robertson, I.M., Birnbaum, H.K. (1990) *Acta Metall.* 38, 2031-2040.
31. Ferreira, P.J., Robertson, I.M., Birnbaum, H.K. (1998) *Acta Metall.* 46, 1749-1757.
32. Valiente, A., Caballero, L., Ruiz, J. (1999) *Nucl. Eng. Design* 188, 203-216.
33. Nagumo, M., Nakamura, M., Takai, K. (2001) *Metall. Mater. Trans.* 32A, 339-347.
34. Matsuo, T., Honma, N., Matsuoka, S., Murakami, Y. (2008) *Trans. JSME.* A74-744, 1164-1173.
35. Tanaka, H., Honma, N., Matsuoka, S., Murakami, Y. (2007) *Trans. JSME*. A73-736, 1358-1365.
36. Kanezaki, T., Narazaki, C., Mine, Y., Matsuoka, S., Murakami Y. (2008) *Int. J. Hydrogen Energy.* 33, 2604-2619.
37. Laird, C. (1967) *ASTM STP*, 415, 131-168.
38. Pelloux, R. M. N. (1969) *Trans. ASM*. 62, 281-285.
39. Neumann, P. (1974) *Acta Metall.* 22, 1155-1165.
40. Bichler, C.H., Pippan, R. (1999) In: *Engineering Against Fatigue*, pp.211-218, Beynon, J.H. and others (Ed.)., Balkema, Rotterdam,.
41. Sofronis, P., McMeeking, R.M. (1989) *J. Mech. Phys. Solids.* 37, 317-350.
42. Murakami, Y., Kanezaki, T., Mine, Y., Matsuoka, S. (2008) *Metallurgical and Materials Trans.*, 39A, 1327-1339
43. Elber, W. (1971) *ASTM STP*. 486, 230-242.
44. Ritchie, R.O., Suresh, S., Moss, C.M. (1980) *Trans. ASME, J. Eng. Mater. Tech.* 102, 293-299.
45. Minakawa, K., McEvily, A.J. (1981) *Scripta Metall.* 15, 633-636.
46. Toplosky, J., Ritchie, R.O. (1981) *Scripta Metall.* 15, 905-908.
47. Suresh, S., Ritchie, R.O. (1983) *Eng. Fract. Mech.* 18, 785-800.